Thermal evolution of vacancy-type defects in quenched FeCrNi alloys

C. X. Zhang [1, 2], X. Z. Cao [2], Y. H. Li [1], S. X. Jin [2], E. Y. Lu [2], H. W. T [2], P. Zhang [2], B. Y. Wang [2, *]

[1] School of Nuclear Science and Technology, Lanzhou University, Lanzhou 730000, China

[2] Key Laboratory of Nuclear Radiation and Nuclear Energy Technology, Institute of High Energy Physics, Chinese Academy of Sciences, Beijing, 100049, China

Abstract

The effect of isochronal annealing on vacancy-type defects in quenched FeCrNi alloys and SUS316 has been investigated by positron annihilation techniques. Vacancy-type defects gather and grow with the annealing temperature increasing to 523 K, and the vacancy-type defects annihilated gradually in FeCrNi alloys at the annealing temperature increasing. The results indicate that the addition of Mo and nonmetal elements is not the key reasons that determined the annihilated temperature of vacancy-type defects. It's worth noting that the vacancy-type defects annihilated and dislocation-type defects formed in all sample alloys after 673 K annealing treatment. In addition, the density of defects in Mo diluted FeCrNi model alloy is lower than that in FeCrNi model alloy due to the Mo-vacancy complexes formed in Mo diluted FeCrNi model alloy. The long lifetime of vacancy-type defects in commercial stainless steel SUS316 is smaller than that in FeCrNi model alloys because the mobility of vacancy-type defects changed by nonmetal elements. In addition, vacancy-type and dislocation defects detected contribute to the S and W parameters of positron annihilation in the whole annealing treatment.

Keywords (positron annihilation, vacancy-type defects, FeCrNi alloy, dislocation, Mo diluted)

1 Introduction

FeCrNi ternary model alloy has been investigated extensively due to the radiation resistance of FeCrNi based austenitic stainless steel as a promising structural material of fission reactor and fusion reactor in recent years [1, 2]. The hardness and embrittlement of structural materials caused by the migration and gathering of radiation-induced defects play an important role in shortening the service lifetime of nuclear reactor [1-7]. The void growth of defect structures under neutron irradiated in FeCrNi austenitic stainless steels shown that the defect formation behaviors during that period strongly depend on alloy composition, especially the minor element in commercial alloy [4]. And the point defect processes in neutron irradiated FeCrNi model alloy and Ti-added modified FeCrNi model alloy indicated that complex defects type formed in alloys, such as stacking fault tetrahedral, dislocation and precipitants [5]. Unfortunately, considered to the mechanism of vacancy-type defects structural evolution and the effect of minor element Mo and C are still unclearly, it is necessary to investigate the thermal evolution process of vacancy-type defects in FeCrNi model alloy. And more importantly, it is difficult to investigate these micro mechanism because the complicated chemical composition exists in commercial austenite stainless steels [8]. Nevertheless, FeCrNi ternary model alloy is the matrix alloy of austenite stainless steels, and these main elements play a decisive role to determine the property of austenite stainless steels [2, 9, 10]. Usually, FeCrNi ternary model alloy is selected to investigate the mechanism of vacancy annihilation to avoid the effect of complex chemical composition in experiments, especially for the primeval mechanism and thermal dynamics of vacancy-type defects induced by irradiation.

Positron annihilation spectroscopy is a powerful nondestructive technique for detecting vacancy-type

* Corresponding author: wangboy@ihep.ac.cn

defects in metal materials. Positron annihilation lifetime spectroscopy could reflect the information of the size and density of vacancy-type defects. Doppler broadening spectroscopy could reflect useful information about the distribution of elements around the annihilation site [11, 12]. Especially the type, size and density of the defects, Mo-vacancy complexes could be reflected by positron annihilation spectroscopy in this work.

In this study, the thermal evolution of vacancy-type defects in quenched Fe17Cr12Ni has been studied. In order to research the interactional effect of Mo element and nonmetal element with vacancy-type defects, Fe17Cr12Ni2Mo model alloy and SUS316 also have been investigated.

2 Experimental

2.1 Materials and preparation

In experiment, Fe17Cr12Ni and Fe17Cr12Ni2Mo model alloys were melted from high purity Fe (99.995%), Cr (99.999%) and Ni (99.995%) in a vacuum induction furnace at 1873 K, where the composition was in wt%. SUS316 steel was commercial austenite stainless steel, which supplied by China Iron & Steel Research Institute Group. The chemical compositions of three kind specimens are listed in Table 1. All specimens, with size of 0.3 mm thick and 1.0 mm×1.0 mm square, were annealed at 1323 K for 2 h in a vacuum and air-cooled to room temperature, and quenched from 1323 K in ice water. Before isochronal annealed treatment performed, all specimens were electrochemically polished. Isochronal annealed treatment experiments were carried out from 293 K to 923 K for 0.5 h in vacuum with a 50 K increment.

Table 1 Chemical compositions of the FeCrNi alloys and SUS316 (wt. %).

Alloys	Fe	Cr	Ni	Mo	C	Si	P	Mn
Fe17Cr12Ni	Bal.	16.78	12.13					
Fe17Cr12Ni2Mo	Bal.	17.12	12.42	1.55				
SUS316	Bal.	16.08	10.08	2.03	0.068	0.354	0.035	1.12

2.2 Positron annihilation measurement

The positron annihilation measurements were performed after specimens annealed. The radioactivity of ^{22}Na positron source is about 1.0×10^{6} Bq, was sandwiched between two same specimens and each spectrum was accumulated to a total count of 2.0×10^{6} to reduce statistical error. The positron lifetime spectrometer has a time resolution of 196 ps (full width at a half maximum) using a slow-fast coincidence system. To make a distinction between bulk and other defects (dislocations, vacancies et al.), the spectra of quenched specimens were decomposed into two components as the short lifetime (τ_1) and long lifetime (τ_2) after subtracting the source and back ground components. The mean lifetime (τ_m) reflects the total amount of vacancy-type defects [13]. The long lifetime (τ_2) conveys the information of the size of vacancy-type defects, and the intensity (I_2) corresponds to the density of the vacancy-type defects, in this present work, mainly vacancy-type clusters and microvoids in FeCrNi [13]. The short lifetime τ_1 originates the positron lifetime of free electrons and interstitial type defects [2, 14, 15].

Doppler Broadening Spectra (DBS) were measured by a single HPGe detector. In the spectrum, the S parameter is defined as positron annihilation with low-momentum ($|P_L| < 3.0\times10^{-3}\ m_0c$) valence electrons, and the W parameter comes from positron annihilations with core electrons in the high-momentum region ($13.0\times10^{-3}\ m_0c < |P_L| < 30.0\times10^{-3}\ m_0c$). The W parameter represents characteristic

signals that positron annihilation with the outer layer valence electron and the S parameter conveys the information that positron annihilation with the free electron in alloys.

3 Results

Figure 1 show the positron annihilation lifetimes and the corresponding intensities in quenched model alloy Fe17Cr12Ni, Fe17Cr12Ni2Mo and SUS316 dependent the annealing temperature. In figures, the long lifetimes (τ_2) in quenched Fe17Cr12Ni, Fe17Cr12Ni2Mo and SUS316 is 313.2 ps 310.4 ps and 287.3 ps, respectively. The long lifetime slightly increases with the annealing temperatures increasing from 423 K to 523 K, and they are turn to decrease as the temperature over 523 K. It indicates that the size of the vacancy-type defects enlarge with annealing temperature increasing from 423 K to 523 K. On the other hand, the few changes of I_2 at temperatures from 423 K to 523 K in all specimens illustrates that the changes of the vacancy-type defects density are not obvious. It's worth noting that the long lifetimes for all specimens decrease rapidly at the annealing temperature range of 523 K - 673 K. In addition, the increments of the long lifetime intensities ($\triangle I_2$) from 623 K to 673 K were 25.9%, 13.1% and 18.6% is corresponding to the samples Fe17Cr12Ni, Fe17Cr12Ni2Mo and SUS316, respectively. It suggests that the density of vacancy-type defects in the Fe17Cr12Ni2Mo is lower than that in Fe17Cr12Ni and SUS316, because vacancy-type defects occupied by Mo atoms or Mo-vacancy complexes formed in Mo diluted FeCrNi model alloy. With the annealing temperature increasing from 673 K to 923 K, the long lifetimes in all the specimens are closing to 170 ps, that is larger than 110 ps for the positrons annihilation lifetime in FeCrNi model alloy matrix [10], which demonstrates that the another type defect formed. Wang et al. had reported that dislocation-type defects formed after vacancy-type defects annihilated in quenched FeCrNi model alloy due to the larger vacancy-type clusters collapsed at higher temperature annealing treatment [16]. Thus, the values of the long lifetime indicate that the dislocation-type defects may be formed in samples. Meanwhile, the long lifetime intensities decrease at annealing temperatures from 723 K to 923 K. It shows that the defects annihilated in all samples. The changes of the mean lifetimes (τ_m) are not obvious at the annealing temperature from 293 K to 523 K. τ_m decreases directly from 165 ps to 115 ps with the annealing temperature increasing from 523K to 673 K.

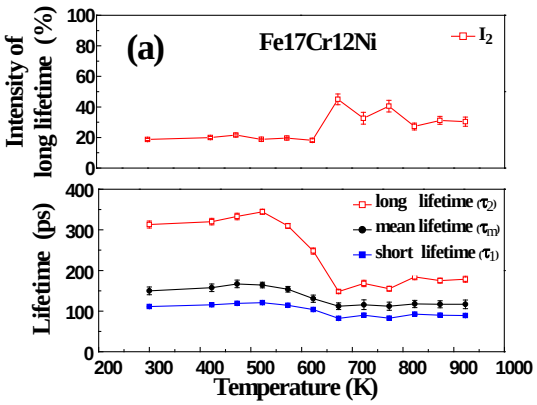

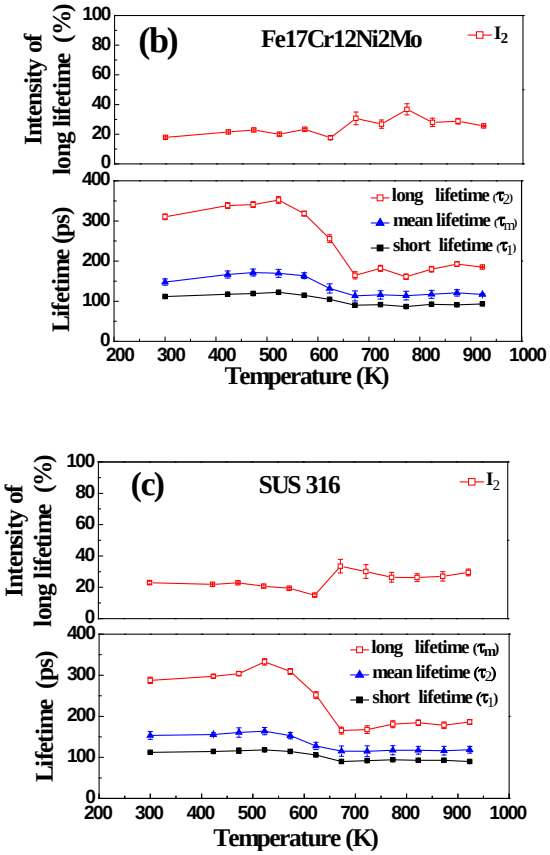

Figure 1 Positron annihilation lifetimes with the isochronal annealing temperature in quenched model alloy Fe17Cr12Ni (a), Fe17Cr12Ni2Mo (b) and SUS316 (c).

The changes of S parameter for Fe17Cr12Ni, Fe17Cr12Ni2Mo and SUS316 with annealing temperature are shown in figure 2. The value of S parameter gradually decreases with the temperature increasing from 293 K to 623 K. The S parameter in quenched specimens is $S_{SUS316} > S_{Fe17Cr12Ni} > S_{Fe17Cr12Ni2Mo}$ at the same annealing temperature. Noteworthily, S parameters closing to same value (0.43) as the temperature increases over 673 K, which indicates that the vacancy-type defects annihilated. According to the long life time results at the higher annealing temperature (> 673 K), the S parameter over 673 K is contributed by the positron annihilation at dislocation.

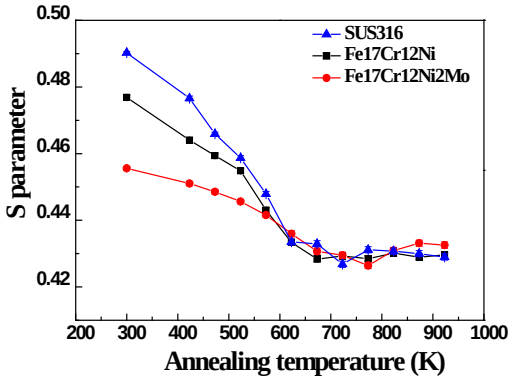

Figure 2 S parameters with the annealing temperature in quenched model alloy Fe17Cr12Ni, Fe17Cr12Ni2Mo and SUS316.

S-W plots with annealing temperature are shown in figure 3. In which, the point (1, 1′, 1″), (2, 2′, 2″), (3, 3′, 3″), (4, 4′, 4″), (5, 5′, 5″) and (6, 6′, 6″) is corresponding to the temperature 293 K, 423 K, 473 K, 523 K, 573 K and 623 K, respectively. These points are aligned on three separate lines for different specimens marked by L, L′ and L″ with different slops corresponding to Fe17Cr12Ni, Fe17Cr12Ni2Mo and SUS316. The difference of L′ and L slopes is very small compare with L″. It indicates that the mechanism of positron annihilation is different between model alloys and commercial alloys. The effect of Mo element addition can be negligible in model alloys for the thermal evolution of vacancy-type defects. With the annealing temperature increases to 673 K, S-W plots close to same point, and the slopes change to same value as the temperature increasing from 673 K to 923 K. As well know, S-W plot can be used to identify the number of defect type in materials, because every kind of positron annihilation site is characterized by a typical (S, W) couple [17]. The results significantly indicate that the dislocation-type defects formed in all samples, and it contribute to the S and W parameters of positron annihilation in the higher annealing treatment, as the slopes changed at 673 K.

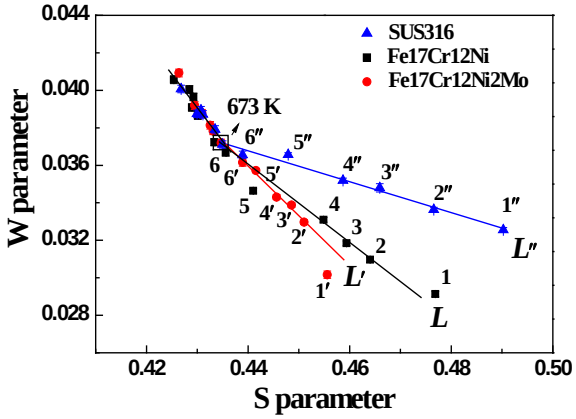

Figure 3 S-W curves in Fe17Cr12Ni, Fe17Cr12Ni2Mo and SUS316 with the different annealing temperature were marked with L, L′ and L″, respectively. The points of (1, 1′, 1″), (2, 2′, 2″), (3, 3′, 3″), (4, 4′, 4″), (5, 5′, 5″) and (6, 6′, 6″) are corresponding to the temperature points 293 K, 423 K, 473 K, 523 K, 573 K and 623 K.

4 Discussions

The long lifetime in quenched specimens is significantly larger than the lifetime value of the single vacancy (~ 178 ps). It shows that the vacancy-type defects of complex size produced in quenched specimens, more like vacancy clusters are introduced into specimens (~ 310 ps in model alloys and 290 ps in SUS316). Compare with model alloys, the long lifetime is smaller, and the S parameter is higher at the annealing temperature from 293 K to 623 K in SUS316. Due to the nonmetal impurity elements exist in SUS316, such as Si, C and P. Si element could change the mobility of vacancy-type defects by interacting with vacancy-type defects [8]. And In fact, when C atoms exist in alloys, C would suppress the growth of the vacancy-type clusters because of vacancy-type defects could be strongly attracted by C element and vacancy-carbon pairs are rather stable [8, 18, 19].

However, the increment of long lifetime intensity in Fe17Cr12Ni2Mo (only 13.1%) is less than that in Fe17Cr12Ni and SUS316 at the recovery stage (523 K - 673 K) of vacancy-type defects. These

indicate the addition of Mo element would suppress the formation of vacancy-type defects in FeCrNi model alloys. Further, the S values at the annealing temperatures from 293 K to 623 K in Fe17Cr12Ni2Mo alloy is lowest (i. e., $S_{Fe17Cr12Ni2Mo} < S_{Fe17Cr12Ni} < S_{SUS316}$ at the same annealing temperature). This results show that the vacancy-type defects occupied by Mo atoms or Mo-vacancy complexes. It further demonstrates that the bonding energy of vacancy-type defects and Mo is lower than Fe, Cr, and Ni. This conclusion is consistent with the simulated results of complexes bonding energy (vacancy and metal atoms such as Fe, Cr, Ni, Mo) [20, 21]. Therefore, Mo atoms are easily combines with the vacancy-type defects and form the Mo-vacancy complexes. Thus, the results of lifetime and S parameters reveal that the density of defects in Mo diluted FeCrNi model alloy is lower than that in FeCrNi model alloys and SUS316. And thus, there are a large number of Mo-vacancy complexes in quenched Mo diluted FeCrNi model alloy [16].

The values of S-W slope in FeCrNi model alloys are higher than that in SUS316 (figure 3) at the lower annealing temperature range of 293 K-623 K, and the values of S-W slopes are not obvious in Fe17Cr12Ni and Fe17Cr12Ni2Mo. It indicates that the effect of nonmetal element is larger than Mo element addition in specimens. At the higher annealing temperature range of 673 K-923 K, the S-W curves turning to same linear function in three alloys, which means that there are the same positrons annihilation mechanisms at higher annealing temperature range for all specimens, as the dislocation-type defects formed. Because the samples underwent a process of recrystallization after vacancy-type defects annihilated due to the vacancy-type clusters collapsed [16, 22]. And importantly, the turning temperature is 673 K for positron lifetime, S parameters and S-W plots in all samples. It further indicates that the addition of Mo and nonmetal could not affect the annihilated temperature of vacancy-type defects. On the other hand, the S-W curves results indicate that there are two different types defect, vacancy-type defects and dislocation-type defects, contribute to the S and W parameters of positron annihilation in the whole annealing treatment.

5 Conclusions

In the present work, the thermal evolution of vacancy-type defects in quenched FeCrNi alloys with the annealing temperature has been investigated. There are a number of vacancy-type defect clusters introduced by quenching. The vacancy-type defects gradually annihilated at the annealing temperature range 523 K - 673 K. And the results of positron annihilation lifetime and Doppler broadening may illustrate that the formation of dislocation due to the vacancy-type clusters collapsed in all alloys after 673 K annealing treatment. On the other hand, compare with nonmetal elements, the affect of Mo element addition was slightly that determines the vacancy-type defects annihilated mechanism, but the minor element could not affect the vacancy-type defects annihilated temperature in samples. The density of vacancy-type defects in Mo diluted FeCrNi model alloy is lower than that in FeCrNi model alloy due to the existence of Mo-vacancy complexes in Mo diluted FeCrNi model alloy. The size of vacancy-type defects in SUS316 is smaller than that in FeCrNi model alloys, because nonmetal element could change the mobility of vacancy-type defects in SUS316.

Acknowledgements This work was supported by the National Natural Science Foundation of China, under Grant No. 91226103 and 91026006.

References

[1] C. Sun, Y. Yang, Y. Liu, K.T. Hartwig, H. Wang, S.A. Maloy, T.R. Allen, X. Zhang, Thermal

stability of ultrafine grained Fe–Cr–Ni alloy, Mater. Sci. Eng., A, 542 (2012) 64-70.
[2] E. Kuramoto, T. Tsutsumi, K. Ueno, M. Ohmura, Y. Kamimura, Positron lifetime calculations on vacancy clusters and dislocations in Ni and Fe, Comput. Mater. Sci., 14 (1999) 28-35.
[3] C. Sun, K.Y. Yu, J.H. Lee, Y. Liu, H. Wang, L. Shao, S.A. Maloy, K.T. Hartwig, X. Zhang, Enhanced radiation tolerance of ultrafine grained Fe–Cr–Ni alloy, J. Nucl. Mater., 420 (2012) 235-240.
[4] T. Yoshiie, K. Sato, X. Cao, Q. Xu, M. Horiki, T.D. Troev, Defect structures before steady-state void growth in austenitic stainless steels, J. Nucl. Mater., 429 (2012) 185-189.
[5] M. Horiki, T. Yoshiie, K. Sato, Q. Xu, Point defect processes in neutron irradiated Ni, Fe–15Cr–16Ni and Ti-added modified SUS316SS, Philos. Mag., 93 (2013) 1701-1714.
[6] S. Zhu, Y. Zheng, D. Yuan, Y. Zuo, P. Fan, D. Zhou, Q. Zhang, X. Ma, B. Cui, L. Chen, W. Jiang, Y. Wu, Q. Wang, L. Peng, X. Cao, B. Wang, L. Wei, Effect of triple ion beams on radiation damage in CLAM steel, AIP Conf. Proc., 1533 (2013) 179-183.
[7] K.L. Wong, H.-J. Lee, J.-H. Shim, B. Sadigh, B.D. Wirth, Multiscale modeling of point defect interactions in Fe–Cr alloys, J. Nucl. Mater., 386-388 (2009) 227-230.
[8] M. Lambrecht, A. Almazouzi, Positron annihilation in neutron irradiated iron-based materials, J. Phys: Conf. Ser., 265 (2011) 012009.
[9] R. Wang, X. Liu, A. Ren, J. Jiang, C. Xu, P. Huang, Y. Wu, C. Zhang, X. Wang, Proton-irradiation-induced damage in Fe–0.3wt.%Cu alloys characterized by positron annihilation and nanoindentation, Nucl. Instrum. Methods Phys. Res., Sect. B, 307 (2013) 545-551.
[10] M. Horiki, T. Yoshiie, S.S. Huang, K. Sato, X.Z. Cao, Q. Xu, T.D. Troev, Effects of alloying elements on defect structures in the incubation period for void swelling in austenitic stainless steels, J. Nucl. Mater., 442 (2013) S813-S816.
[11] S.M. He, N.H. van Dijk, H. Schut, E.R. Peekstok, S. van der Zwaag, Thermally activated precipitation at deformation-induced defects in Fe-Cu and Fe-Cu-B-N alloys studied by positron annihilation spectroscopy, Phys. Rev. B, 81 (2010).
[12] S. Novy, P. Pareige, C. Pareige, Atomic scale analysis and phase separation understanding in a thermally aged Fe–20at.%Cr alloy, J. Nucl. Mater., 384 (2009) 96-102.
[13] T. Ishizaki, Q. Xu, T. Yoshiie, S. Nagata, The recovery of gas-vacancy-complexes in Fe irradiated with high energy H or He ions, Mater Trans, 45 (2004) 9-12.
[14] Y. Nagai, K. Takadate, Z. Tang, H. Ohkubo, H. Sunaga, H. Takizawa, M. Hasegawa, Positron annihilation study of vacancy-solute complex evolution in Fe-based alloys, Phys. Rev. B, 67 (2003).
[15] H. Wu, X. Cao, G. Cheng, J. Wu, J. Yang, P. Zhang, Z. Li, A.Z.M.S. Rahman, R. Yu, B. Wang, Effects of copper precipitates on microdefects in deformed Fe-1.5 wt%Cu alloy, Phys. Status Solidi A, 210 (2013) 1758-1761.
[16] B. Y. Wang, S. H. Zhang, T.M. Wang, Recovery behaviour of quenched-in defects in Fe-Cr-Ni alloy by positron annihilaton, Acta Metallurgica Sinica, 33 (1997) 271-276.
[17] J. Qiu, Y. Xin, X. Ju, L.P. Guo, B.Y. Wang, Y.R. Zhong, Q.Y. Huang, Y.C. Wu, Investigation by slow positron beam of defects in CLAM steel induced by helium and hydrogen implantation, Nucl. Instrum. Methods Phys. Res., Sect. B, 267 (2009) 3162-3165.
[18] S.I. Porollo, S.V. Shulepin, Y.V. Konobeev, F.A. Garner, Influence of silicon on swelling and microstructure in Russian austenitic stainless steel EI-847 irradiated to high neutron doses, J. Nucl. Mater., 378 (2008) 17-24.
[19] M. Lambrecht, L. Malerba, Positron annihilation spectroscopy on binary Fe–Cr alloys and

ferritic/martensitic steels after neutron irradiation, Acta Mater., 59 (2011) 6547-6555.
[20] M J Puska, R.M. Nieminen, Defect spectroscopy with positrons: a general calculational method, J. Phys. F: Met. Phys, 13 (1983) 333-346.
[21] H. Ohkubo, Z. Tang, Y. Nagai, M. Hasegawa, T. Tawara, M. Kiritani, Positron annihilation study of vacancy-type defects in high-speed deformed Ni, Cu and Fe, Mater. Sci. Eng., A, 350 (2003) 95-101.
[22] T. Yoshiie, X. Cao, Q. Xu, K. Sato, T.D. Troev, Damage structures in austenitic stainless steels during incubation period of void swelling, Phys. Status Solidi A, 6 (2009) 2333-2335.